

MAGDALENA URBANIAK

Szczecin University of Technology  
 Department of Mechanics and Machine Elements  
 Al. Piastow 19, Szczecin 70-310, Poland  
 e-mail: magdalena.urbaniak@ps.pl

## Glass transition temperature-temperature-property ( $T_gTP$ ) diagram for EPY<sup>®</sup> epoxy system

**Summary** — Evolution of storage and loss moduli during conversion progress of the filled epoxy system EPY<sup>®</sup> (Epidian 6 with triethylenetetramine), applied for the production of machine foundation chocks, was studied using dynamic mechanical thermal analysis (DMTA). The results obtained and the results previously reached by differential scanning calorimetry (DSC) and rotational viscometry made possible to determine the diagram glass transition temperature-temperature-property ( $T_gTP$ ) for the investigated system, where  $T_g$  is the direct measure of conversion and P denotes property under investigation — loss modulus. This way of using  $T_g$  in this diagram makes possible the linearization of the relationships among the temperatures corresponding to the maxima and minima of the physical properties and the extent of cure. The lines within  $T_gTP$  diagram show the courses of structural transformations during cure *i.e.* glass transition ( $T_g$ ),  $\beta$ -transition ( $T_\beta$ ) and gelation ( $_{gel}T_g$ ). The diagram lines separate several regions which are dependent on the extent of cure and the material shows different physical properties within each of them.  $T_gTP$  diagram calculated for the EPY<sup>®</sup> material can facilitate understanding of the relationships among transitions and material properties.

**Key words:** epoxy system, extent of cure, gelation, glass transition, loss modulus,  $T_gTP$  diagram.

### DIAGRAM TEMPERATURA ZESZKLENIA–TEMPERATURA–WŁAŚCIWOŚĆ ( $T_gTP$ ) UKŁADU EPOKSYDOWEGO EPY<sup>®</sup>

**Streszczenie** — Metodą termicznej analizy dynamicznych właściwości mechanicznych (DMTA) badano zmiany modułu zachowawczego ( $E'$ ) i modułu stratności ( $E''$ ) z postępem konwersji (rys. 3, 4 i 5) napełnionego układu epoksydowego EPY<sup>®</sup> (Epidian 6 z trietylenotetraaminą). Materiał ten jest stosowany do produkcji podkładek fundamentowych maszyn. Wyniki tych badań razem z wynikami uzyskanymi wcześniej za pomocą różnicowej kalorymetrii skaningowej (DSC) (tabela 1) i wiskozymetrii rotacyjnej pozwoliły na wyznaczenie diagramu temperatura zeszklenia-temperatura-właściwość ( $T_gTP$ ) tego układu (rys. 1, 2 i 6), gdzie  $T_g$  jest bezpośrednią miarą postępu konwersji, a P oznacza rozpatrywaną właściwość — moduł stratności. Użycie  $T_g$  jako bezpośredniej miary postępu konwersji w tym diagramie umożliwiła linearyzację zależności między wartościami temperatury odpowiadającymi maximum i minimum właściwości fizycznych a postępem sieciowania. Linie na diagramie  $T_gTP$  odzwierciedlają przebieg przemian strukturalnych materiału: zeszklenie ( $T_g$ ),  $\beta$ -przejście ( $T_\beta$ ) i żelowanie ( $_{gel}T_g$ ). Linie te wyznaczają również podobszary, w których materiał, w miarę postępu konwersji, wykazuje różne właściwości fizyczne. Opracowany diagram  $T_gTP$  tworzywa EPY<sup>®</sup> umożliwił lepsze zrozumienie zależności między przemianami zachodzącymi w układzie a właściwościami materiału.

**Słowa kluczowe:** układ epoksydowy, postęp reakcji sieciowania, żelowanie, zeszklenie, moduł stratności, diagram  $T_gTP$ .

Epoxy resins are the most important thermosetting polymers, widely used as structural adhesives, composite materials, surface coatings, electronic devices [1–5]. The chemical reactions occurring during the cure of epoxy resins cause physical changes associated with the two distinct macroscopic transitions of gelation and vitrification [6–8].

Gelation is a sudden and irreversible transformation of the system from a viscous liquid to an elastic gel. It

corresponds to the incipient formation of an infinite network at the first stage of curing, causing changes in macroscopic properties of the system. Gelation occurs at a definite conversion for a system (according to the Flory's theory of gelation) and it depends on the functionality of the epoxy resin and stoichiometry of the components [9, 10].

Vitrification involves a physical transformation from a liquid or rubbery state to a glassy state as a result of an

increase in crosslinking density of the material. This phenomenon occurs when glass transition temperature ( $T_g$ ) becomes equal to the curing temperature ( $T_c$ ). The vitrification point marks a change in the reaction mechanism passing from chemically kinetically-controlled to diffusion-controlled one. From that point the reaction becomes slow and finally stops [11, 12].

These transitions occurring during cure reaction of epoxy resins can be studied using different techniques. A detailed review of thermal analysis techniques applicable to epoxy characterization is available in literature [2]. Gelation and vitrification can be conveniently determined by dynamic mechanical analysis (DMA). Although vitrification is commonly determined by DMA, differential scanning calorimetry (DSC) offers increased temperature accuracy and control [13]. A combination of these two techniques allows separation of gelation and vitrification [13] and provides the information necessary describing a cure diagram. There are analytical equations describing the cure progress of epoxy systems as functions of both temperature and time [14] which allow verification of a cure diagram.

Occurrence of both these transitions is caused by increasing extent of cure for thermoset system within the cure time. A growing extent of cure is related with non-linear increase in  $T_g$  because at a small extent of cure, the increase in  $T_g$  is due to increasing molecular weight of epoxy resin, whereas, at a high extent of cure, an increasing  $T_g$  results in higher crosslinking densities [15].

Determination of the thermal conditions in which these transitions occur makes a basis for developing the cure diagrams useful in practice *i.e.* time-temperature-transition (*TTT*) diagram, conversion-temperature-transition (*CTT*) diagram and also glass transition temperature-temperature-property ( $T_gTP$ ) diagram discussed in this article. These diagrams facilitate grasping and understanding the relationships among reactants, cure path, transformations, structure, physical states and properties of the material. *TTT* and *CTT* cure diagrams calculated for the EPY<sup>®</sup> epoxy system were presented in previous articles [16, 17].

However, in this article  $T_gTP$  diagram is presented where *P* can denote a specified property of the material (*e.g.*, loss modulus, density, physical ageing rate).  $T_gTP$  diagram (presented schematically in Fig. 1) creates a general framework for understanding and summarizing the relationships among the properties and the extent of cure at various temperatures from the liquid state to the glassy state [18, 19].

The X-axis and Y-axis of the  $T_gTP$  diagram (Fig. 1) are the extent of cure (as measured by  $T_g$ ) and the temperature of the system ( $T$ ), respectively. Straight lines in the diagram determine the conversion relating to the values of specific temperatures of the system, *i.e.*  $T_g$ , the onset ( $iT_g$ ) and the end ( $eT_g$ ) temperature of the glass transition as well as  $\beta$ -transition ( $T_\beta$ ) temperature and also gelation temperature ( $_{gel}T_g$ ). The whole area of the diagram is

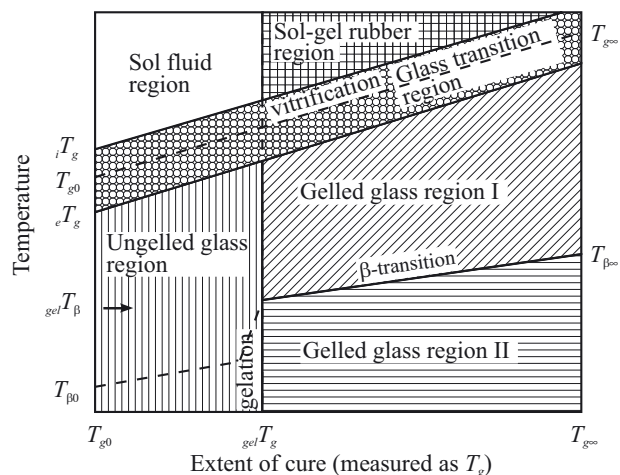


Fig. 1. Schematic glass transition temperature-temperature-property ( $T_gTP$ ) diagram for thermosetting systems; designations — see the text

divided by these lines into several regions which are related to various stages of the cured material, *i.e.* ungelled glass, gelled glass I, gelled glass II, glass transition, sol fluid, and sol-gel rubber. The diagram developed in this way is aimed at visualization of the conversion effect of the system (measured as  $T_g$  values) on isothermal properties of the material. The regions marked in  $T_gTP$  diagram show that structural changes of the system occur as cure proceeds. The lines of the diagram allow to indicate the maxima and minima of the selected properties relating to conversion of the system. Hence  $T_gTP$  diagram makes possible to qualify the behavior of the physical properties of the material with respect to increasing cure of the system determined by its temperature and its  $T_g$  [18].

$T_gTP$  diagram is analogous to *TTT* diagram [20], except that it deals with properties after cure rather than during the cure. The Y-axis (indicating the measured temperature) is identical in both diagrams. However, different values can be seen on the X-axis which show the glass transition temperature ( $T_g$ ) in  $T_gTP$  diagram and the cure time in *TTT* diagram. Thanks to that the X-axis distinctly differentiates presentation of conversion in both of the diagrams. The extent of cure is shown in *TTT* and  $T_gTP$  diagrams through iso-conversion curves and outright in the X-axis, respectively. Since  $T_g$  is uniquely related to fractional conversion and can be measured more accurately than the letter especially at high conversion [11] hence measured  $T_g$  value is the most sensitive indicator of the changes in network structure. Then  $T_g$  is directly related not only to the solidification process and the state of the material but it is involving to the network structure and material properties as well. Furthermore, physical properties of the epoxy system deep in glassy state (*e.g.* density, modulus and physical ageing rate) versus extent of cure are determined principally by the values of variables  $T_g$  and  $T$

[18] and changes of these properties are affected by  $T_g$  and  $T_\beta$  both of which grow along with the increase in the extent of cure.

The EPY<sup>®</sup> epoxy system — the object of the investigations presented in this and earlier papers [16, 17] — is applied as a material for the foundation chocks in seating of a ship machinery and installations and also for many various heavy land-based machines [21].

The main aim of this study was to develop a  $T_gTP$  diagram for the epoxy material where loss modulus is the property analyzed therein. The diagram developed in such a way can be a basis for analysis of the correlation of the changes occurring along with an increase in the extent of conversion so the casual connection between the structure and properties of the material.

## EXPERIMENTAL

### Materials

The main components of the investigated material, which trade name is EPY<sup>®</sup> (from Marine Service Jaroszewicz, Szczecin, Poland) are: epoxy resin Epidian 6 (epoxy number 0.532 mole/100 g) and a curing agent Z-1 (triethylenetetramine), both produced by Chemical Works Organika-Sarzyna in Nowa Sarzyna, Poland. The resin and curing agent ratio is constant and equals 14 parts of the curing agent per 100 parts of the resin. The epoxy system is completed with additives giving appropriate technological and useful properties of the material. The chemical structures of the reacting materials are shown in the previous article [22].

### Sample preparation

The system samples were cast in steel forms in the shape of rectangular bars (50×10×5 mm) and cured at 23 °C for 24, 48 or 168 h. Besides, several samples cured at 23 °C for 24 h were additionally postcured at 40, 60, 80 or 100 °C for 2 h. Preparation of the samples used in the investigations of gelation and postcuring processes was given in the previous article [16].

### Methods of testing

#### DSC measurements

Differential scanning calorimeter (Du Pont DSC 910) was used to follow the postcuring. The DSC technique has been well described in the literature [23, 24]. Parameters now applied were the same as defined in the previous article [16].

#### Viscoelastic measurements

Parallel plate rheometry was used to measure the material behavior below the gel point. Viscoelastic data were obtained using ARES rheometer (Rheometric

Scientific) and were the same as defined in the previous article [16]. The rotational viscometry technique has been well described in the literature [25, 26].

#### DMTA measurements

Dynamic mechanical thermal analysis (DMTA) enables to define both elastic and viscous flow characteristics of viscoelastic materials [27—29]. An example of the former is the storage modulus ( $E'$ ), of the latter the loss modulus ( $E''$ ). Tangent delta =  $E''/E'$  is also in use. DMTA MK-II dynamic thermal analyzer (from Polymer Laboratories) in three-point bending mode was used. The specimen was cooled with rate 5 °C/min from room temperature to -100 °C under the nitrogen atmosphere and then heated with rate 3 °C/min from -100 to 250 °C and subjected to oscillating frequency of 1 Hz. Evolution of  $E'$  and  $E''$  moduli was registered during the temperature-scanning experiments. The temperatures at which various relaxations occur, *i.e.*  $T_\beta$  and  $T_g$  were determined during heating. Temperature of  $\beta$ -relaxation ( $T_\beta$ ) is associated with localized subsegmental motions of  $\beta$ -transition below  $T_g$  whereas  $T_g$  — with cooperative or segmental motions of glass transition. The temperatures of the maxima in  $E''$  modulus attained at low- and high-temperature part of the scan on heating were used to assign the values of  $T_\beta$  and  $T_g$ , respectively.

It is noticeable that DMTA gives higher  $T_g$  values than DSC due to the measurement of extrinsic mechanical properties rather than intrinsic heat capacity and the poorer temperature control of the instrument [30]. For this reason the  $E''$  maxima values were just used to determine the  $T_g$  values because the latter would be approximately 15 °C higher if the tangent delta maxima were applied for the same purpose.

### Development of $T_gTP$ diagram

An experimental development of  $T_gTP$  diagram for thermoset resins performed only on the grounds of experimental results involved costly and time consuming experimental measurements. In the previous article [16] it was proved that the number of necessary experimental measurements can be limited to a minimum thanks to numerical modeling. This modeling allows determination of both the conversion at the gel point ( $\alpha_{gel}$ ) and the temperature at which gelation and vitrification of the investigated system occur simultaneously ( $_{gel}T_g$ ). These measurement results obtained with the use of dynamic and isothermal DSC and rotational viscometry (ARES) were completed with the results presented in this article which comprise the runs of storage modulus ( $E'$ ) and loss modulus ( $E''$ ) changes obtained using dynamic mechanical thermal analysis (DMTA) method. The flow chart for development of  $T_gTP$  diagram is shown in Fig. 2. An appropriate gathering and combining of the experimental results allow to develop  $T_gTP$  diagram for the material.

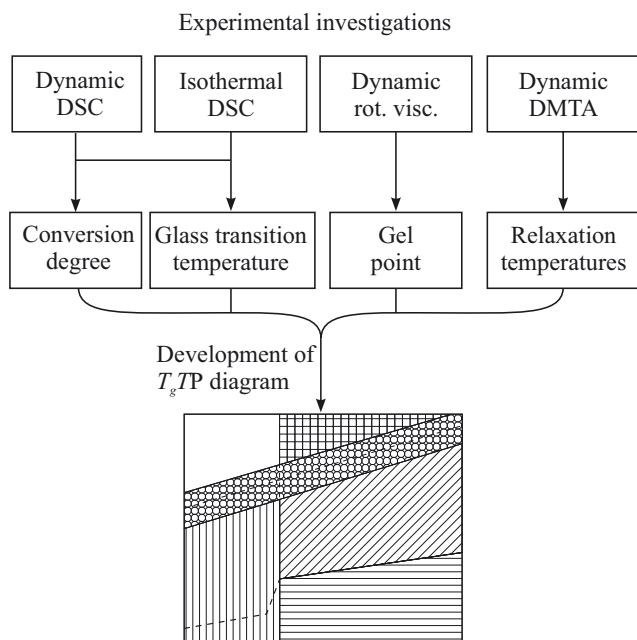


Fig. 2. Flow chart of the experimental development of  $T_gTP$  diagram

## RESULTS AND DISCUSSION

### Principal parameters of the epoxy-amine system

The characteristic glass transition temperatures of the EPY<sup>®</sup> system which were determined in the way given in the previous article [16] are included in Table 1, where  $T_{g0}$  and  $T_{g\infty}$  are the glass transition temperature of the uncured material and glass transition temperature of the fully cured material, respectively. Value of the conversion degree at the gel point ( $\alpha_{gel}$ ) and value of the temperature at which gelation and vitrification occur simultaneously ( $_{gel}T_g$ ) are also included in this Table. Value of the  $_{gel}T_g$  was calculated using the DiBenedetto's equation [31] and value of the  $\alpha_{gel} = 0.58$  was determined experimentally.

Table 1. Principal parameters for EPY<sup>®</sup> system [16]; description of symbols — see the text

$\alpha_{gel}$	$T_{g0}$ , °C	$_{gel}T_g$ , °C	$T_{g\infty}$ , °C	$T_{\beta\infty}$ , °C
0.58	-45.6	12.5	111.2	-35.5

The relaxation temperatures of the system corresponding to the maxima in loss modulus ( $E''$ ) versus temperature were determined using the DMTA technique with frequency of 1 Hz. The  $\beta$ -relaxation temperature ( $T_{\beta\infty}$ ) of the fully cured EPY<sup>®</sup> material is included in Table 1.

The principal parameters:  $T_{g0}$ ,  $T_{g\infty}$ ,  $T_{\beta\infty}$ ,  $\alpha_{gel}$  and  $_{gel}T_g$  make a basis for description of the complex behavior of the properties of thermoset systems after cure versus

chemical conversion [32]. Such a description can be provided in the form of  $T_gTP$  diagram.

### $T_g$ versus conversion

The relation between  $T_g$  and progress of conversion for the material which was verified in the previous article [16] showed good agreement of the experimentally obtained results with DiBenedetto's model. These results confirmed that  $T_g$  value proved to be a good index for monitoring of chemical conversion.

### Transitions during temperature scans versus extent of cure

The thermomechanical properties, *i.e.* storage modulus ( $E'$ ) and loss modulus ( $E''$ ), obtained during temperature scans for the material cured to different extents, are shown in Figs. 3a and b, respectively.

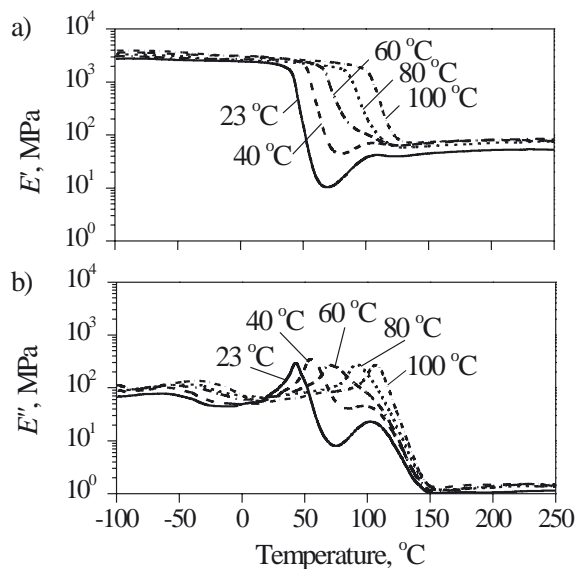


Fig. 3. Temperature dependence of storage modulus  $E'$  (a) and loss modulus  $E''$  (b) for the EPY<sup>®</sup> material postcured at various temperatures

$T_g$  that grows because of the curing from  $T_{g0}$  to  $T_{g\infty}$  is reflected by the maximum of dominant relaxation peak at the loss modulus ( $E''$ ) curve shown in Fig. 3b. The areas under the peaks of  $E''$  modulus diminish and become narrower along with the increase in postcure temperature. A reduction in the breadth of such a peak is a symptom of contraction of the temperature interval in which glass transition occurs whereas more and more small area of the peak shows an increase in conversion for the material along with an increase in postcure temperature.

Below  $T_g$ , a small peak at low temperature part of the modulus  $E''$  curve is observed and its maximum determines the  $\beta$ -relaxation temperature ( $T_\beta$ ) combined with



flexible subsegments of the developing network.  $T_\beta$  of the system grows with increasing conversion which is shown in Fig. 3b.

**$T_g$  versus  $T_\beta$**

A temperature scan of the material from the liquid or rubbery state into the glassy state yields the temperatures of the glass transition ( $T_g$ ) and secondary transition ( $T_\beta$ ) for the system. The values of  $T_g$  and  $T_\beta$  were determined from the loss modulus ( $E''$ ) maxima at low and high temperature parts of the scan, respectively. It is shown in Fig. 3b that values of  $T_g$  and  $T_\beta$  of the system increase along with extent of cure throughout the curing process.

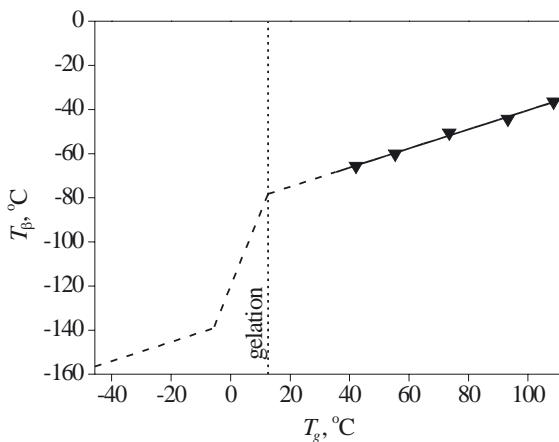


Fig. 4. Dependence of  $T_\beta$  on  $T_g$  (as measure of extent of cure) for the EPY<sup>®</sup> material

Dependence of  $T_\beta$  on  $T_g$  (considered as measure of conversion) described in the literature [18] shows a jump in the vicinity of gelation (Fig. 4). This may be indicative of different micromechanisms of  $\beta$ -transition before and after gelation. However, it can also be seen (Fig. 4) that  $T_\beta$  increases linearly with  $T_g$  as before so after the gel point. It seems that the changes of  $T_\beta$  and  $T_g$  are affected by similar structural factors, i.e. the crosslinking sites after gelation [18, 33]. The  $\beta$ -transition temperature of the system at its gel point is defined here as  $_{gel}T_\beta = -78.3$  °C (Fig. 4). This temperature is a material parameter of a curing system similarly as  $T_g$  of the curing system at its gel point,  $_{gel}T_g = 12.5$  °C and both are independent on curing temperature [9, 18]. An increase in  $T_\beta$  after gel point, with an increasing extent of cure, significantly affects physical properties of the system in glassy state [18].

**$E'$  modulus versus extent of cure**

The investigation results of thermomechanical behavior of the material postcured at various temperatures (from 40 to 100 °C) thus brought to different values of conversion extent, are shown in Fig. 5. This figure clearly

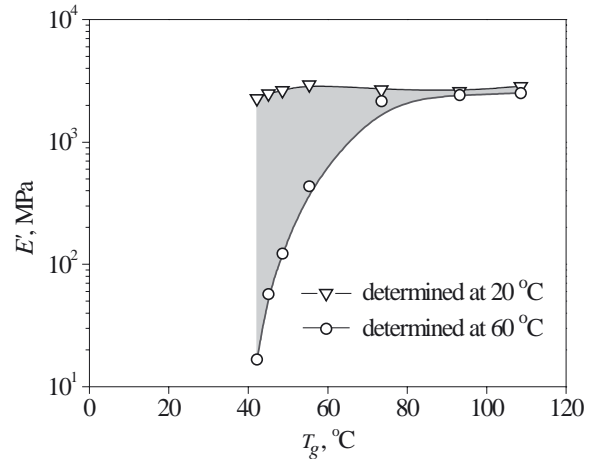


Fig. 5. Evolution of storage modulus ( $E'$ ) versus extent of cure for the EPY<sup>®</sup> material

shows the variation scope of storage modulus ( $E'$ ) for such postcured material which was determined (on the basis of Fig. 3a) at temperatures of 20 and 60 °C corresponding to the typical values of working temperature for foundation chocks of main and auxiliary ship's engines. The picture of  $E'$  modulus variation shown in such a way distinctly indicates that also a rise in its resistance to softening occurs along with an increase in postcure temperature of the material. On this ground (Fig. 5) from a practical point of view one can assume that the optimal postcure temperature for the EPY<sup>®</sup> material approximately equals 80 °C. This temperature not only can secure an elimination of risk of the material softening in the working temperature range for foundation chocks but it can also ensure obtaining stable measurement values of  $E'$  modulus.

**$T_g$ -temperature-property ( $T_g$ TP) diagram**

The results obtained of the epoxy system were summarized in the form of the  $T_g$ TP diagram (Fig. 6), where

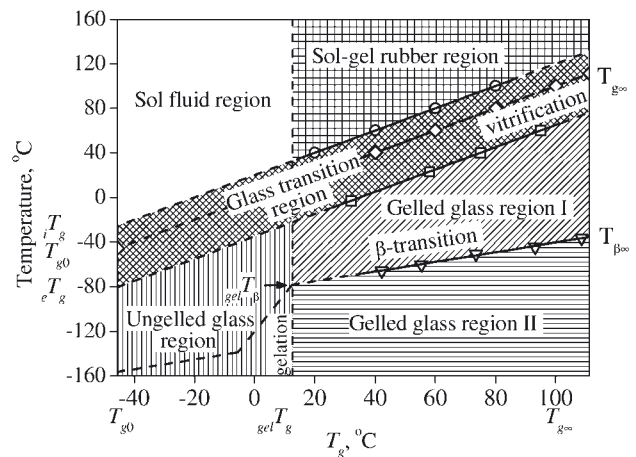


Fig. 6.  $T_g$ TP diagram ( $P$  is  $E''$  modulus) developed experimentally for the EPY<sup>®</sup> material

P denotes specified property of the material and here it stands for loss modulus ( $E''$ ). The X-axis and Y-axis of the diagram are conversion measured by  $T_g$  and temperature of the system, respectively.

To plot the diagram it was necessary to determine experimentally some of the characteristic temperatures of the system, *i.e.*  $T_{g0} = -45.6$  °C,  $T_{g\infty} = 111.2$  °C. Other necessary temperature at which gelation and vitrification occur simultaneously  $_{gel}T_g = 12.5$  °C was calculated using DiBenedetto's equation, whereas the value of  $\alpha_{gel} = 0.58$  was determined experimentally [16].

The major transitions, gelation and vitrification, which affect material properties are illustrated by straight lines in  $T_g$ TP diagram. Gelation is represented as a vertical dashed line in the diagram separating the sol and sol/gel regions at  $_{gel}T_g = 12.5$  °C whereas vitrification shows a solid diagonal line, corresponding to  $T_g = T$ . There are also two straight lines denoting the onset ( $_iT_g \approx T_g - 20$  °C) and the end ( $_eT_g \approx T_g + 35$  °C) temperatures of the glass transition. Besides the diagram makes visible the course of  $\beta$ -transition temperature ( $T_\beta$ ) versus extent of cure with dash broken line and solid diagonal one in the range of low and high extent of cure, respectively.

$T_g$ TP diagram area is separated by the above mentioned lines into several regions of different extent of cure at the selected cure temperature for the epoxy system. The cured material shows different physical properties in each of these regions. To introduce oneself to the material properties at various temperatures in the aspect of changing of loss modulus values one can distinguish the following regions in  $T_g$ TP diagram:

— **Ungelled glass region** ( $T < _eT_g$  and  $T_{g0} < T_g < _{gel}T_g$ )  
— isothermal modulus of the material increases linearly and sharply along with increasing extent of cure.

— **Gelled glass region I** ( $T_\beta < T < _eT_g$  and  $_{gel}T_g < T_g < T_{g\infty}$ ) — isothermal modulus of the material decreases along with increasing extent of cure.

— **Gelled glass region II** ( $T < T_\beta$  and  $_{gel}T_g < T_g < T_{g\infty}$ )  
— isothermal modulus of the material increases at a low rate along with increasing extent of cure relative to that in the ungelled glass region.

— **Glass transition region** ( $_eT_g < T < _iT_g$  and  $T_{g0} < T_g < T_{g\infty}$ ) — modulus of the material shows a large progressive increase along with increasing extent of cure due to vitrification, attaining a maximum at  $_eT_g$ , beyond vitrification. Glass transition region includes three lines in  $T_g$ TP diagram corresponding to the onset of glass transition ( $_iT_g \approx T_g - 20$  °C), to vitrification ( $T_g = T_c$ ), and to the end of glass transition ( $_eT_g \approx T_g + 35$  °C).

— **Sol fluid region** ( $T > T_g$  and  $T_{g0} < T_g < _{gel}T_g$ ) — the material is a viscous fluid with low modulus. The modulus shows a small step-increase near the gel point along with increasing extent of cure [18, 33].

— **Sol-gel rubber region** ( $T > T_g$  and  $_{gel}T_g < T_g < T_{g\infty}$ )  
— modulus increases along with increasing extent of cure.

The significance of  $T_g$ TP diagram is that the critical points (such as the maximum and minimum of modulus versus extent of cure) are arranged linearly and almost parallelly to the vitrification ( $T_g$ ) line. These arrangements indicate that the properties of thermoset materials in glassy state seem to be determined mostly by the values of variables  $T_g$  and  $T$  applied to the material. The use of  $T_g$  as a measure of extent of cure results in linearization of the relationships among the critical points and temperature in  $T_g$ TP diagram. This facilitates the construction of  $T_g$ TP diagrams for different systems [18].

## CONCLUSION

$T_g$ TP diagram calculated for the EPY<sup>®</sup> epoxy material is a valuable complement to the cure diagrams *i.e.* TTT isothermal cure diagram [16] and CTT diagram described previously [17]. All the diagrams are useful and suitable tools for deeper understanding of the relationships among the reactants, cure path, structures, transformations, physical states and properties of the material.

## REFERENCES

1. "Epoxy Resins. Chemistry and Technology", (Ed. May C. A.), 2<sup>nd</sup> edition, Marcel Dekker, New York 1988, pp. 653—928.
2. Bilyeu B., Brostow W., Menard K. P.: *J. Mater. Ed.* 1999, **21**, 281.
3. Bilyeu B., Brostow W., Menard K. P.: *J. Mater. Ed.* 2000, **22**, 109.
4. Bilyeu B., Brostow W., Menard K. P.: *J. Mater. Ed.* 2001, **23**, 189.
5. Mazela W., Czub P., Pielichowski J.: *Polimery* 2004, **49**, 231.
6. Pascault J. -P., Sautereau H., Verdu J., Williams R. J. J.: "Thermosetting Polymers", Marcel Dekker, New York 2002, pp. 67—145.
7. Williams R. J. J.: "Transitions during network formation", in "Polymer Networks: Principles of their Formation, Structure and Properties", (Ed. Stepto R. F. T.), Blackie Academic & Professional, Chapman & Hall, London 1998, pp. 93—124.
8. Friedrich K., Ulański J., Boiteux G., Seytre G.: *Polimery* 2006, **51**, 648.
9. Flory P. J.: "Principles of Polymer Chemistry", Cornell University Press, Ithaca, New York 1953, pp. 347—361.
10. Plazek D. J., Frund Z. N.: *J. Polym. Sci. Polym. Phys.* 1990, **28**, 431.
11. Wisanrakkit G., Gillham J. K.: *J. Appl. Polym. Sci.* 1990, **41**, 2885.
12. Guibe C., Francillette J.: *J. Appl. Polym. Sci.* 1996, **62**, 1941.
13. Bilyeu B., Brostow W., Menard K. P.: *Polym. Compos.* 2002, **23**, 1111.
14. Brostow W., Glass N. M.: *Mat. Res. Innovat.* 2003, **7**, 125.

15. Keenan M. R.: *J. Appl. Polym. Sci.* 1987, **33**, 1725.
16. Urbaniak M., Grudziński K.: *Polimery* 2007, **52**, 117.
17. Urbaniak M., Grudziński K.: *Polimery* 2007, **52**, 255.
18. Wang X., Gillham J. K.: *J. Appl. Polym. Sci.* 1993, **47**, 425.
19. Gillham J. K., Enns J. B.: *Trends Polym. Sci.* 1994, **2**, 406.
20. Enns J. B., Gillham J. K.: *J. Appl. Polym. Sci.* 1983, **28**, 2567.
21. Grudziński K., Jaroszewicz W.: "Seating of machines and devices on foundation chocks cast of EPY resin compound", ZAPOL Publisher, Szczecin 2004, pp. 19—32.
22. Urbaniak M., Grudziński K.: *Polimery* 2004, **49**, 89.
23. Höhne G. W. H., Hemminger W. F., Flammersheim H. J.: "Differential Scanning Calorimetry. An Introduction for Practitioners", 2<sup>nd</sup> edition, Springer-Verlag, Berlin 2003.
24. Barton J. M.: "Epoxy Resins and Composites I", in "Advances in Polymer Science", vol. 72, (Ed. Dušek K.) Springer-Verlag, Berlin 1985, pp. 112—154.
25. Macosko Ch. W.: "Rheology: Principles, Measurements, and Applications", Wiley-VCH, New York 1994.
26. Laza J. M., Julian C. A., Larrauri E., Rodriguez M., Leon L. M.: *Polymer* 1998, **40**, 35.
27. Menard K. P.: "Dynamic Mechanical Analysis: A Practical Introduction", CRC Press, Boca Raton 1999.
28. Menard K. P.: "Thermal transitions and their measurement", in "Performance of Plastics", (Ed. Brostow W.), Ch. 8, Hanser, Munich — Cincinnati 2000.
29. Lucas E. F., Soares B. G., Monteiro E.: "Caracterização de Polímeros — Determinação de Peso Molecular e Análise Térmica", e-papers Serviços Editoriais, Rio de Janeiro 2001.
30. O'Neal H. R., Welch S., Guilford S., Curran G., Menard K. P., Rogers J.: *J. Adv. Mater.* 1995, **26**, 49.
31. Pascault J. P., Williams R. J.: *J. Polym. Sci. Polym. Phys.* 1990, **28**, 85.
32. Venditti R. A., Gillham J. K.: *J. Appl. Polym. Sci.* 1995, **56**, 1687.
33. Enns J. B., Gillham J. K.: *J. Appl. Polym. Sci.* 1983, **28**, 2831.

Received 2 IV 2007.